



# Magnetically Promoted Rapid Immunofluorescence Staining for Frozen Tissue Sections

**Tatsuya Onishi, Sachiko Matsuda, Yuki Nakamura, Junko Kuramoto, Akinori Tsuruma, Satoshi Sakamoto, Shunichi Suzuki, Daiichiro Fuchimoto, Akira Onishi, Shinichi Chikaki, Miki Kaneko, Akihiro Kuwahata, Masaki Sekino, Hiroshi Yasuno, Naohiro Hanyu, Tomoko Kurita, Hiroyuki Takei, Takashi Sakatani, Kanae Taruno, Seigo Nakamura, Tetsu Hayashida, Hiromitsu Jinno, Moriaki Kusakabe, Hiroshi Handa, Kaori Kameyama, and Yuko Kitagawa**

Department of Surgery (TO, SM, YN, TH, YK) and Department of Pathology (JK), Keio University School of Medicine, Tokyo, Japan; Department of Breast Surgery, National Cancer Center Hospital East, Kashiwa, Japan (TO); School of Life Science and Technology, Tokyo Institute of Technology, Yokohama, Japan (AT, SSakamoto); Division of Animal Sciences, Institute of Agrobiological Sciences, National Agriculture and Food Research Organization, Tsukuba, Japan (SSuzuki, DF); Laboratory of Animal Reproduction, Department of Animal Science and Resources, College of Bioresource Sciences, Nihon University, Fujisawa, Japan (AO); Graduate School of Engineering (SC, MKaneko, AK, MS) and Graduate School of Agricultural and Life Sciences (MKusakabe), The University of Tokyo, Tokyo, Japan; Tamagawa Seiki Co. Ltd., Nagano, Japan (HY, NH); Department of Breast Surgery, Nippon Medical School, Tokyo, Japan (TK, HT); Department of Diagnostic Pathology, Nippon Medical School Hospital, Tokyo, Japan (TS); Division of Breast Surgical Oncology, Showa University, Tokyo, Japan (KT, SN); Department of Surgery, Teikyo University School of Medicine, Tokyo, Japan (HJ); Matrix Cell Research Institute Inc., Ushiku, Japan (MKusakabe); Department of Nanoparticle Translational Research, Tokyo Medical University, Tokyo, Japan (HH); and Department of Diagnostic Pathology, Keio University Hospital, Tokyo, Japan (KK)

## Summary

Current immunohistochemistry methods for diagnosing abnormal cells, such as cancer cells, require multiple steps and can be relatively slow compared with intraoperative frozen hematoxylin and eosin staining, and are therefore rarely used for intraoperative examination. Thus, there is a need for novel rapid detection methods. We previously demonstrated that functionalized fluorescent ferrite beads (FF beads) magnetically promoted rapid immunoreactions. The aim of this study was to improve the magnetically promoted rapid immunoreaction method using antibody-coated FF beads and a magnet subjected to a magnetic field. Using frozen sections of xenograft samples of A431 human epidermoid cancer cells that express high levels of epidermal growth factor receptor (EGFR) and anti-EGFR antibody-coated FF beads, we reduced the magnetically promoted immunohistochemistry procedure to a 1-min reaction and 1-min wash. We also determined the optimum magnetic force for the antibody reaction (from  $7.79 \times 10^{-15}$  N to  $3.35 \times 10^{-15}$  N) and washing ( $4.78 \times 10^{-16}$  N), which are important steps in this technique. Furthermore, we stained paraffin-embedded tissue arrays and frozen sections of metastatic breast cancer lymph nodes with anti-pan-cytokeratin antibody-coated FF beads to validate the utility of this system in clinical specimens. Under optimal conditions, this ultra-rapid immunostaining method may provide an ancillary method for pathological diagnosis during surgery. (J Histochem Cytochem 67: 575–587, 2019)

## Keywords

cancer, fluorescent ferrite beads, immunostaining, intraoperative diagnosis, magnetic field

## Introduction

Immunohistochemistry (IHC) staining is widely used for diagnosing abnormal cells such as those found in cancerous tissue. Antibodies bind specifically to

Received for publication September 29, 2018; accepted March 7, 2019.

### Corresponding Author:

Sachiko Matsuda, Department of Surgery, Keio University School of Medicine, 35 Shinanomachi, Shinjuku-ku, Tokyo 160-8582, Japan.

E-mail: matsuda-sa@umin.ac.jp

**Table 1.** Current Rapid Immunostaining Protocol for Frozen Sections.

	Ultrasound	Microwave	A/C	One Step Immunofluorescence	Magnetically Promoted Rapid Immunofluorescence
Fixation	2 min <sup>a</sup>	2 min <sup>a</sup>	2 min <sup>a</sup>	3 min <sup>b</sup>	5 min <sup>c</sup>
Washing			0.5 min <sup>d</sup>	2.0 min <sup>e</sup>	
Blocking	0.5 min <sup>f</sup>	0.5 min <sup>f</sup>			5 min <sup>g</sup>
Primary antibody	1.5 min	5 min	2 min	3–5 min	1 min
Washing	0.25 min <sup>h</sup>	0.25 min <sup>h</sup>	0.5 min <sup>d</sup>	1.5 min <sup>d</sup>	1 min
Secondary antibody	1.5 min	5 min	2 min <sup>i</sup>		
Washing	0.25 min <sup>h</sup>	0.25 min <sup>h</sup>	0.5 min <sup>d</sup>		
Reaction with substrate	1 min <sup>j</sup>	1 min <sup>j</sup>	3 min <sup>j</sup>		
Counterstaining	0.25 min <sup>k</sup>	0.25 min <sup>k</sup>			

<sup>a</sup>Acetone; <sup>b</sup>EtOH; <sup>c</sup>10% neutral buffered formalin; <sup>d</sup>Phosphate buffered saline; <sup>e</sup>Water; <sup>f</sup>H<sub>2</sub>O<sub>2</sub>; <sup>g</sup>4% skimmed milk; <sup>h</sup>Tris-buffered saline; <sup>i</sup>EnVisionTM + System/HRP Mouse; <sup>j</sup>Diaminobenzene; <sup>k</sup>Hematoxylin.

antigens in biological tissues, and IHC staining can be accomplished by a number of methods. The avidin-biotin complex method is one of the most commonly used IHC staining systems, which involves four sequential steps: (1) primary antibody, (2) biotin-labeled secondary antibody, (3) avidin-biotin-peroxidase complex, and (4) diaminobenzidine (DAB) staining. Hybridization of the primary antibody to the antigen is typically accomplished with conditions that range from overnight at 4C to 15 min at temperatures as high as 37C; conditions are largely dependent on primary antibody affinity.<sup>1</sup>

In clinical practice, intraoperative frozen sections are usually examined with hematoxylin and eosin (HE) staining. To detect small numbers of tumor cells in sentinel lymph nodes or surgical margins, intraoperative IHC staining is desired.<sup>2</sup> To complete the staining during surgery, a number of rapid IHC methods have been reported to reduce the reaction time of these processes.<sup>3–16</sup> For example, ultrasound irradiation shortens the antibody reaction time to 1.5 min,<sup>3</sup> while Hatta et al.<sup>3</sup> reported that in addition to Brownian motion, stirring increased the stochastic collision between antibodies and antigens to enhance bond formation. Other rapid IHC systems also reduce the staining time with a stirring effect created using external energy such as microwaves<sup>4,6,7</sup> or an alternating current electric field,<sup>13,14,17</sup> reducing the method to <20 min (Table 1). However, these methods are indirect and require many steps including secondary antibodies and washing. Nevertheless, a direct method for decreasing the overall reaction time using a fluorescently labeled primary antibody or premixing the primary antibody and secondary antibody omitted the signal amplification process using a secondary antibody (Table 1).

Advances in ferrite nanoparticle technology have permitted the development of detection technologies in biochemical assays, and we previously reported magnetically promoted rapid immunoreactions using functionalized fluorescent ferrite beads (FF beads).<sup>18</sup> FF beads are dispersive functional polymer beads that contain both ferrites (magnetic iron oxide) and fluorescent europium complexes. A specific antibody can be immobilized on FF beads through chemical transformation. The magnet attracts the magnetic beads and accelerates bond formation between the beads and antigens (Fig. 1A), which is followed by washing to remove undesired binding (Fig. 1B). Using the magnetic collection of antibody-coated FF beads, rapid sandwich immunoassay and immunofluorescence staining were achieved within 1 min and 10 min, respectively. As the method has two simple steps of (1) incubation with primary antibody and (2) washing as the signals are amplified by the complex themselves, immunofluorescence images of the antigen-antibody complex can be captured using a fluorescence detector immediately after the FF bead reaction.

The aim of the present study was to improve the magnetically promoted rapid immunostaining method to a 1-min staining and 1-min wash using antibody-coated FF beads and a magnet subjected to a magnetic field for practical applications using xenograft frozen sectioned tissues, and to validate the efficacy of this system in clinical specimens.

## Materials and Methods

### Antibodies

The anti-pan-cytokeratin antibody and IgG control antibody were purchased from Abcam (Cambridge,

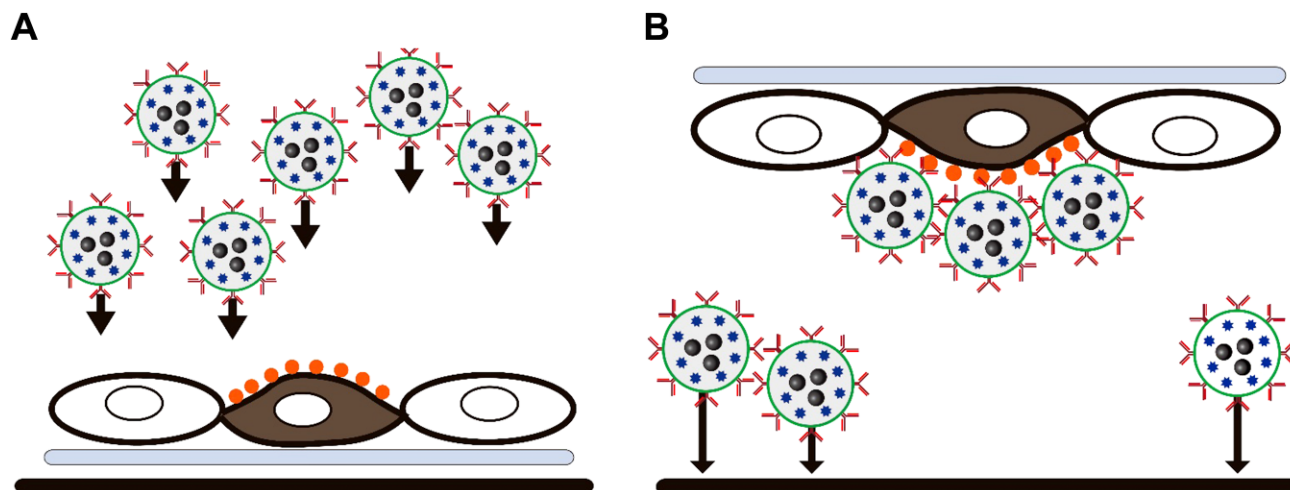


**Figure 1.** Principle of magnetically promoted rapid immunofluorescence (MRIF). Round cell (white): normal cell, spindle cell (brown): malignant cell, orange dots: antigens on the malignant cell, plate (light blue): plate slide, black bar: magnet, red y shape: antibody, blue star shape: fluorescence, black dots: ferrite, black arrow: direction of magnetic force. (A) The magnet attracts the beads to the cells and accelerates the binding with fluorescent ferrite (FF) beads and the antigens. (B) Nonspecific adherence is removed by magnetic force.

UK). The anti-epidermal growth factor receptor (EGFR) antibody was prepared as follows. The hybridoma cell line 528 (HB-8509), which produces mouse monoclonal antibody against EGFR, was obtained from the American Type Culture Collection (ATCC, Rockville, MD) and was cultured with RPMI 1640 medium supplemented with 10% (w/v) heat-inactivated fetal bovine serum (Gibson, Grand Island, NY) in a humidified atmosphere consisting of 5% (v/v) CO<sub>2</sub> in air at 37°C. Ascetic fluid was produced by inoculating BALB/c mice intraperitoneally with  $5 \times 10^6$  hybridoma 528 cells. The fluid was collected from mice after 2 to 4 weeks inoculation and centrifuged at 10,000 g for 10 min to remove debris. Purified 528 antibody was prepared using the Mab Trap kit (GE Healthcare, Uppsala, Sweden) in accordance with the manufacturer's instructions.

### Cell Lines

To optimize the magnetic force and staining conditions for this rapid immunostaining system, xenograft samples of A431 human epidermoid cancer cells, which express high levels of EGFR, were used. EGFR is an important disease marker used to investigate various types of malignancy, including breast cancer, as it plays a pivotal role in tumor cell survival and proliferation.<sup>19–21</sup> Epidermoid carcinoma cells A431 (CRL-1555) were obtained from ATCC, and maintained in DMEM supplemented with 10% fetal bovine serum in a 5% CO<sub>2</sub> humidified incubator at 37°C.

### Xenograft Induction

A431 cells ( $1 \times 10^6$  cells) in 1 ml phosphate buffered saline (PBS) were subcutaneously implanted into the legs of recombination activating gene 2 (RAG2) knockout swine. RAG2 knockout swine lack mature lymphocytes because of their inability to initiate V(D)J rearrangement, leading to immune deficiency.<sup>22</sup> RAG2 knockout swine were coproduced by NARO (Ibaraki, Japan), Prime Tech Ltd (Ibaraki, Japan), and RIKEN (Kanagawa, Japan). The primary tumor was harvested as a positive sample, and superficial lymph nodes were harvested from wild type swine as a negative sample. Tissues were quickly frozen in liquid nitrogen and stored at  $-80^\circ\text{C}$ . All animal experiments were performed with protocols approved by the Ethics Committee of Keio University (approval number: 08073).

### Human Samples

The paraffin-embedded tissue arrays of BRM481 (breast carcinoma metastatic tissue microarray, containing 24 cases of metastatic breast cancer tissue, duplicated cores per case), BRM961 and 961a (breast carcinoma metastatic tissue microarray, containing 48 cases of breast cancer, with 36 matched metastatic breast cancer and 12 normal tissue), LY241e (lymph node and tonsil tissue microarray, containing nine cases of lymph node tissue, plus three cases of normal tonsil tissue, duplicate cores per case), LY481 (lymphatic tissue microarray, including 24 cases of

normal lymphatic tissue, duplicated cores per case), and LY803 (lymph node metastatic adenocarcinoma grade 2–3 tissue microarray of lymph node, 77 cases, and three cases of metastatic signet-ring cell carcinoma, single core per case) were purchased from US Biomax Inc. (Derwood, MD). Detached samples were omitted from analysis. Frozen metastatic lymph nodes were used from six breast cancer patients who underwent lymph node dissection at Showa University Hospital and Nippon Medical School Hospital from February 2018 to October 2018. Patients were given the necessary information about this study, and only lymph nodes from patients who had given consent were used. The dissected metastatic lymph nodes were immediately divided in half. Divided nodes were submitted for clinical examination, and the remaining nodes were frozen in liquid nitrogen and stored at  $-80^{\circ}\text{C}$  for use in this study. This study was conducted based on the ethical principles stated in the Helsinki Declaration of 1975, as revised in 1983. The study was approved by the Human Experimentation Committee of our institutions. The approved numbers are 2377 for Showa University, 29-01-892 for Nippon Medical School, and 2017-0266 for Keio University.

### Preparation of FF Beads

We previously reported unique multifunctional beads in which both fluorophores and ferrite nanoparticles are completely encapsulated in an organic polymer.<sup>23</sup> In brief, we produced  $\text{Eu}(\text{TTA})_3(\text{TOPO})_2$  (where TTA = thenoyltrifluoroacetylacetone and TOPO = tri-*n*-octylphosphine oxide) from europium(III) acetate hydrate, TTA, and TOPO,<sup>24</sup> and novel polymer-coated magnetic beads that have several advantages including homogeneous immobilization of the ligand on the bead surface and magnetic responses.<sup>25,26</sup> Subsequently, a suspension of polymer-coated magnetic beads with carboxylic acid (1.0 mg) was incubated with 10 mmol/l  $\text{Eu}(\text{TTA})_3(\text{TOPO})_2$  solution in acetone in the dark with vigorous shaking for 1 hr at room temperature. Distilled water was added and acetone was evaporated under vacuum at  $60^{\circ}\text{C}$ . After washing the pellet with washing buffer (50 mmol/l HEPES [pH 7.9], 0.1% NP-40), we produced FF beads with a diameter of 200 nm. The FF beads were dispersed in distilled water and stored in the dark at  $4^{\circ}\text{C}$ .<sup>18,24–26</sup>

### Preparation of Antibody-coated FF Beads

A suspension of FF beads with carboxylic acid (1.0 mg) in distilled water was incubated with 60  $\mu\text{l}$  of 50 mg/ml 1-ethyl-3-(3-dimethylaminopropyl) carbodiimide hydrochloride in 2-(*N*-morpholino)ethanesulfonic acid

(pH 6.0) and 60  $\mu\text{l}$  of 50 mg/ml *N*-hydroxysuccinimide in PBS (pH 7.4) for 30 min at room temperature. Subsequently, the activated FF beads were washed with acetate buffer (pH 5.0) and incubated with 1.0 mg/ml of antibody in 80  $\mu\text{l}$  of acetate buffer (pH 5.0) for 2 hr at  $4^{\circ}\text{C}$ . Next, a 1.0 mol/l 2-ethanolamine solution in PBS (pH 8.0) was added and the suspension was mixed overnight at  $4^{\circ}\text{C}$ . Finally, antibody-coated FF beads were washed and stored in PBS containing 0.01% Tween 20 at  $4^{\circ}\text{C}$ . To measure the amount of immobilized antibodies on FF beads, the bicinchoninic acid protein assay was performed according to previously described methods.<sup>27</sup>

### Magnet and Jig

We used a cylindrical magnet (10 mm diameter, 24 mm length; NeoMag, Chiba, Japan) and designed a jig (Fig. 2A) to optimize the distance between the sample and the magnet. The magnet was placed under the specimen stage and the distance was variable.

### Preparation of Fresh Frozen Sections

Approximately  $5 \times 5$  mm chopped samples were embedded in a frozen section compound (Leica, Wetzlar, Germany) and solidified in liquid nitrogen. The frozen samples were sectioned on a cryostat microtome (4–5  $\mu\text{m}$  thick) and mounted onto glass slides (New Silane II; Muto Pure Chemical Co., Ltd., Tokyo, Japan). The specimens were then immersed in five different concentrations and types of fixative solutions including 4% paraformaldehyde solution, 10% neutral buffered formalin, cold acetone, 100% methanol, and 1% acetic acid in 95% ethanol for 5 min at room temperature, and rinsed with PBS. Clinical specimens for pan cytokeratin were immersed in 10% neutral buffered formalin, and antigen retrieval was performed by proteinase K (dilution 1:200; Dako Japan, Tokyo, Japan) at  $42^{\circ}\text{C}$  for 5 sec.

### Preparation of Paraffin-embedded Sections

Specimens were deparaffinized in xylol and rehydrated in a descending ethanol series. Specimens for pan cytokeratin were antigen retrieved by proteinase K (Dako Japan) at  $37^{\circ}\text{C}$  for 15 min.

### Magnetically Promoted Rapid Immunofluorescence (MRIF) Staining

Specimens were blocked with four different concentrations and types of reagents, including 5% or 10% bovine serum albumin (BSA) and 4% or 8% skimmed

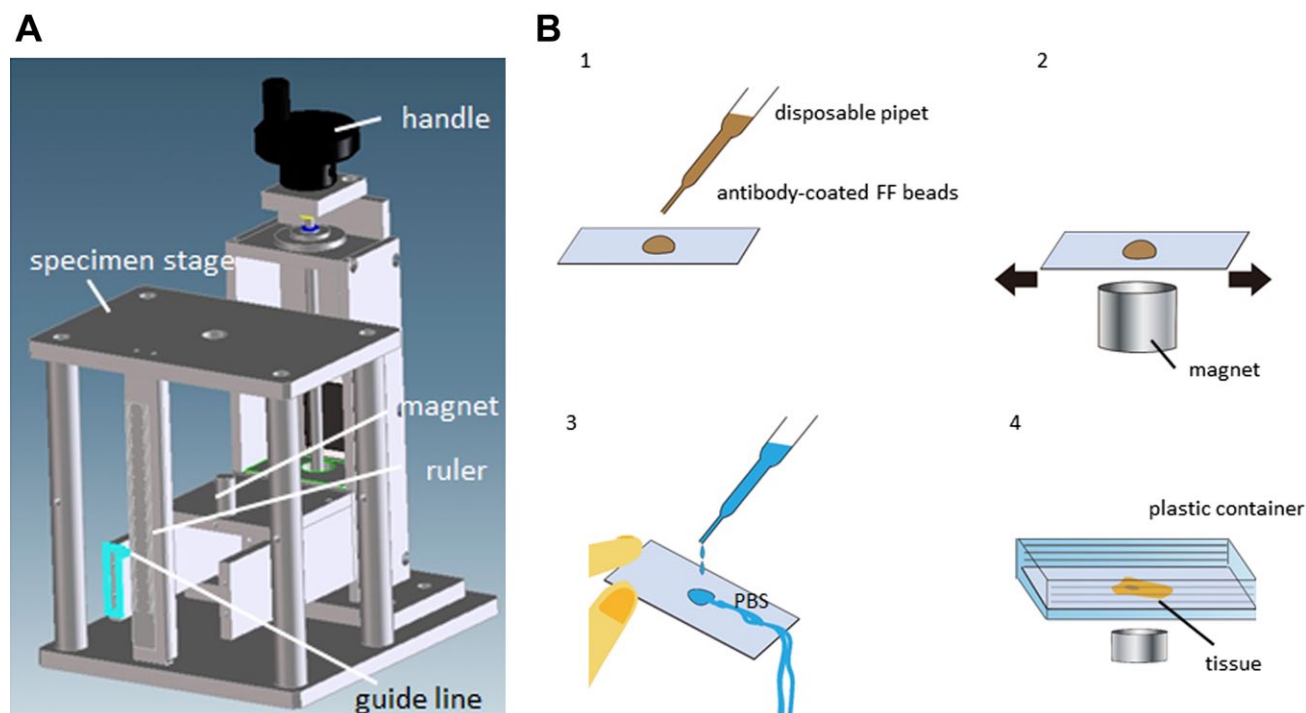


**Figure 2.** The experimental jig and punch picture of MRIF. (A) The handle is used to adjust the distance between the sample and magnet, which can be adjusted to any distance. (B) Scheme of MRIF. Brown liquid: antibody-coated FF beads, blue liquid: phosphate buffered saline (PBS). (1) Drops of diluted FF beads, (2) the slide is vigorously agitated manually above the magnet on the specimen stage of the jig, (3) brief washing with PBS using a disposable pipette, and (4) the slide is inserted into a plastic container and “washed” with a magnet. Abbreviation: FF, fluorescent ferrite; MRIF, magnetically promoted rapid immunofluorescence.

milk in PBS for 5 min. Antibody-coated FF beads were diluted at 1:50 (200  $\mu\text{g}/\text{ml}$ ) with the same blocking solution as the specimens for 20 min before use. The immunostaining punch is shown in Fig. 2B. After removal of the blocking solution, the specimen was incubated with 20  $\mu\text{l}$  antibody-coated FF beads at a 1:50 dilution (200  $\mu\text{g}/\text{ml}$ ) (Fig. 2B1) for 1 min for frozen sections or for 5 min for paraffin embedded sections with a magnetic field beneath the plate. The plate slide was vigorously agitated manually (Fig. 2B2) on the jig. The distance between the sample and magnet was changed from 0 mm to 11 mm at 1 mm intervals. Next, samples were washed with PBS using a disposable pipette (Fig. 2B3), and the slide was placed in a PBS-filled container, sample side down on the magnet to remove the unbound FF beads using a magnetic force for 1 min (Fig. 2B4). The distance between the sample and magnet was changed from 2 mm to 14 mm at 1 mm intervals. The specimens were then gently ejected from the container and mounted with VECTASHIELD Antifade Mounting Medium with DAPI (4',6-diamidino-2-phenylindole). Images were captured using a fluorescence microscope with the filter set ultraviolet

(UV)-1A (Ex. 365/10, Em. long pass; ECLIPS E1000; Nikon, Tokyo, Japan) or NanoZoomer (Hamamatsu photonics K.K., Shizuoka, Japan).

### HE Staining and Conventional IHC Staining Methods

The frozen samples and paraffin-embedded samples were stained by HE in accordance with standard methods and the IHC method. The samples were prepared as described above. For HE staining, the formalin fixed frozen specimens, and deparaffinized and rehydrated paraffin embedded specimens were washed with water, then immersed in Carrazzi's hematoxylin solution for 10 min at room temperature. The samples were briefly rinsed with water followed by differentiation in 1% acid alcohol for 10 sec, and then stained with eosin solution for 7 min.

For the IHC methods, samples were inactivated with endogenous peroxidase in 0.5% periodic acid for 10 min, and blocked in 4% skimmed milk in tris-buffered saline (TBS) for 30 min. After removal of the blocking solution, samples were incubated with the primary antibody as indicated in the blocking solution

(1.0 µg/ml) overnight at 4°C, washed with TBS for 30 min, and then incubated with ENVISION (Dako Japan) for 30 min. After washing with TBS for 30 min, samples were visualized using the DAB reaction for 5 min, counterstained with hematoxylin for 1 min, then dehydrated and mounted onto coverslips.

### Neutralizing Antibody Assay

To confirm the specificity of the antigen and antibody reaction on the magnetically promoted immunoreaction method, A431 xenograft samples were blocked with 10 or 60 ng/µl anti-EGFR antibody overnight at 4°C before the anti-EGFR antibody-coated FF beads were reacted.

### Pathological Analysis

To analyze the reproducibility of the MRIF, the coincidence ratio of the stained site with IHC and MRIF in the specimens were calculated. The calculation was performed by two independent researchers.

## Results

### Calculation of the Magnetic Force

The magnetic force of the cylindrical magnet was calculated to analyze the correlation of magnetic force with immunoreaction. The distribution of the calculated magnetic force,  $F_{abs} = \sqrt{Fz^2 + Fx^2}$ , is shown in Fig. 3A to C. To calculate the magnetic force  $F$ , the distribution of the magnetic field generated by the magnet and the magnetic moment of the FF bead were required. The calculation is shown below, and was performed in MATLAB (The MathWorks, Inc., Natick, MA). The total magnetic moment of the cylindrical magnet is expressed by the summation of the small (0.25 mm<sup>3</sup>) magnet element where 0.25 mm<sup>3</sup> is any number; the magnet is magnetized in the z-direction and the moment of the small magnet  $m_{z0}$  is  $16.35 \times 10^{-6}$  A m<sup>2</sup>. The magnetic flux density ( $Ba$ ) of each element was calculated as follows:

$$Ba = -\frac{\mu_0}{4\pi} \left\{ \frac{m_0}{(r^3)} - \frac{(3(m_0 \cdot r)r)}{(r^5)} \right\}$$

Here,  $r$  is the distance from the element and  $\mu_0$  is the magnetic permeability in a vacuum. The magnetic flux density  $B$  of the cylindrical magnet was calculated by the summation of  $Ba$ . The distribution of the magnetic force was affected by the distance from the magnet and was stronger at the margins than at the center of the magnet.

The magnetic moment ( $m$ ) of a magnetized FF bead is shown in Fig. 3D. The mass ratio of ferrite and polymer was 1:2, the mass densities of ferrite and polymer were 5.0 and 1.1 g/cm<sup>3</sup>, respectively, and the diameter of the FF bead was 200 nm. We obtained the mass of a bead, which was approximately  $6.23 \times 10^{-15}$  g, and the magnetic moment of an FF bead. Therefore, the magnetic force ( $F$ ) acting on an FF bead was calculated as follows:

$$F = mx \left( \frac{dB}{dx} \right) + mz \left( \frac{dB}{dz} \right),$$

assuming the uniform magnetization of the FF beads and axial symmetry.

### Antibody-coated FF Beads and Evaluation of the Stained Images

Before magnetic immunofluorescence staining, the amount of anti-EGFR antibodies immobilized on FF beads was 59.8 µg/mg beads, as calculated using the bicinchoninic acid protein assay.<sup>27</sup> The results of MRIF staining of A431 cells by anti-EGFR antibody-coated FF beads are shown in Fig. 4A. Vivid red fluorescence was observed in the A431 cells treated with anti-EGFR antibody-coated FF beads, indicating that EGFR was specifically stained by MRIF using anti-EGFR antibody-coated FF beads with a magnet. To ensure the specificity of the technique, a swine superficial lymph node was used as a negative control. Only a small number of fluorescent particles were observed in the lymph node in which EGFR was not expressed (Fig. 4B). Fluorescence was negligible in the A431 cells treated with IgG control antibody-coated, antibody-uncoated FF beads, or without the magnet (Fig. 4C).

### Optimization of the MRIF Staining Protocol

We explored the optimal distance between the tissue samples of A431 carcinoma cells and the magnet beneath them at the time of incubation. Anti-EGFR antibody-coated FF beads, but not antibody-uncoated FF beads, bound the tumor cells in 1 min when the distance was within 2 to 5 mm (magnetic force =  $7.79 \times 10^{-15}$  N to  $3.35 \times 10^{-15}$  N). Anti-EGFR antibody-coated FF beads did not adhere to the lymph node tissue in which EGFR was not expressed. When the distance was shorter than 2.0 mm, unwanted background staining was observed in the corresponding negative controls. When the distance was greater than 5 mm, FF beads did not react sufficiently with the samples. These findings indicate that the immunoreaction



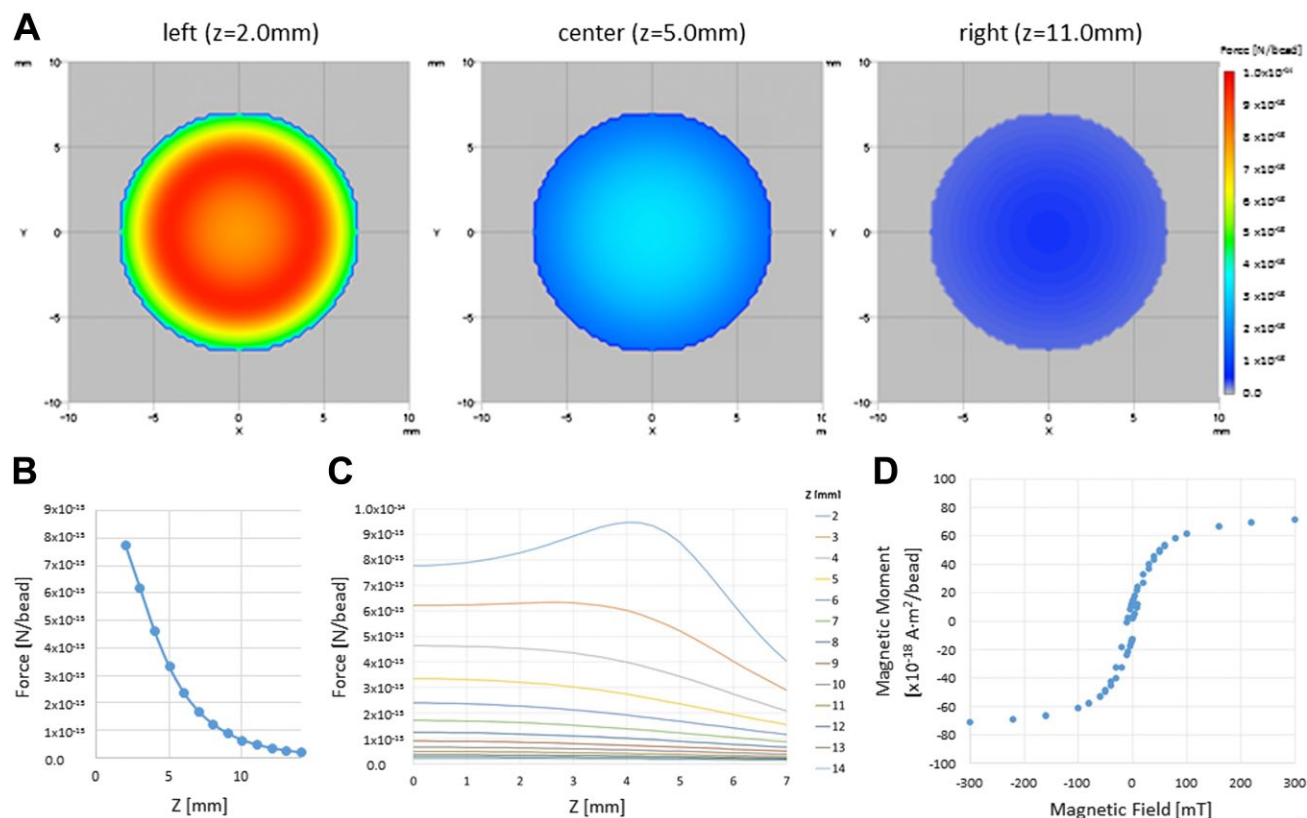


**Figure 3.** The magnetic field strength (force between the cylindrical magnet and FF bead). (A) Color map of the magnetic field strength above the cylindrical magnet with a diameter of 10 mm and a length of 24 mm. Z is the distance from the surface of the magnet. The magnetic strength at various distances above the magnet are shown (left: Z = 2.0 mm, center: Z = 5.0 mm, right: Z = 11 mm). The correspondence between the color and force (N/bead) is shown in the color bar. (B) Log chart of the force between the cylindrical magnet and FF bead. X: Z distance, Y: log (Fabs) [log (N)/bead]. (C) The force between the cylindrical magnet and FF bead by distance from the center for several distances from the magnet. (D) Relationship between magnetic strength B (mT) and magnetic moment of a bead m (A·m<sup>2</sup>). X: applied magnetic strength B (mT), Y: magnetic moment of a bead m (A·m<sup>2</sup>). Abbreviation: FF, fluorescent ferrite.

and magnetic force clearly influence the detection of EGFR.

We also examined the optimal distance for washing. When the distance from the samples to the magnet was 11 mm with a magnetic force of  $4.78 \times 10^{-16}$  N, anti-EGFR antibody-coated FF beads binding to EGFR remained on the A431 tumor tissues. When the distance was >11 mm, unbound FF beads could not be completely washed off the samples. These findings indicate that the magnetic force affects the rinsing of unbound FF beads.

Fixative and blocking conditions also affected the staining. We examined various fixative solutions, including 10% neutral buffered formalin, 4% paraformaldehyde, cold acetone, 100% methanol, and 1% acetic acid in 95% ethanol, with 10% neutral buffered formalin producing the best result. In addition, 4% or 8% skimmed milk and 5% or 10% BSA were examined as blocking solutions, and 4% skimmed milk showed sufficient blocking, whereas BSA was insufficient.

### Staining Images With Neutralizing Antibody

To confirm that this was a specific antigen–antibody reaction, we used anti-EGFR neutralizing antibodies with anti-EGFR antibody-coated FF beads on A431 tumor cells. The fluorescence level was negligible when A431 tumor tissues were blocked with antibody-containing blocking solution, while the fluorescence was bright when it was blocked with antibody-free blocking solution (Fig. 5). These data suggest that the immune reaction of EGFR and antibody-coated FF beads were blocked by the anti-EGFR neutralizing antibody.

### Staining Images of Human Metastatic Lymph Nodes by MRIF Using Pan-cytokeratin Antibody-coated FF Beads

The amount of anti-pan-cytokeratin antibodies immobilized on FF beads was 57.7  $\mu\text{g}/\text{mg}$  beads, as calculated

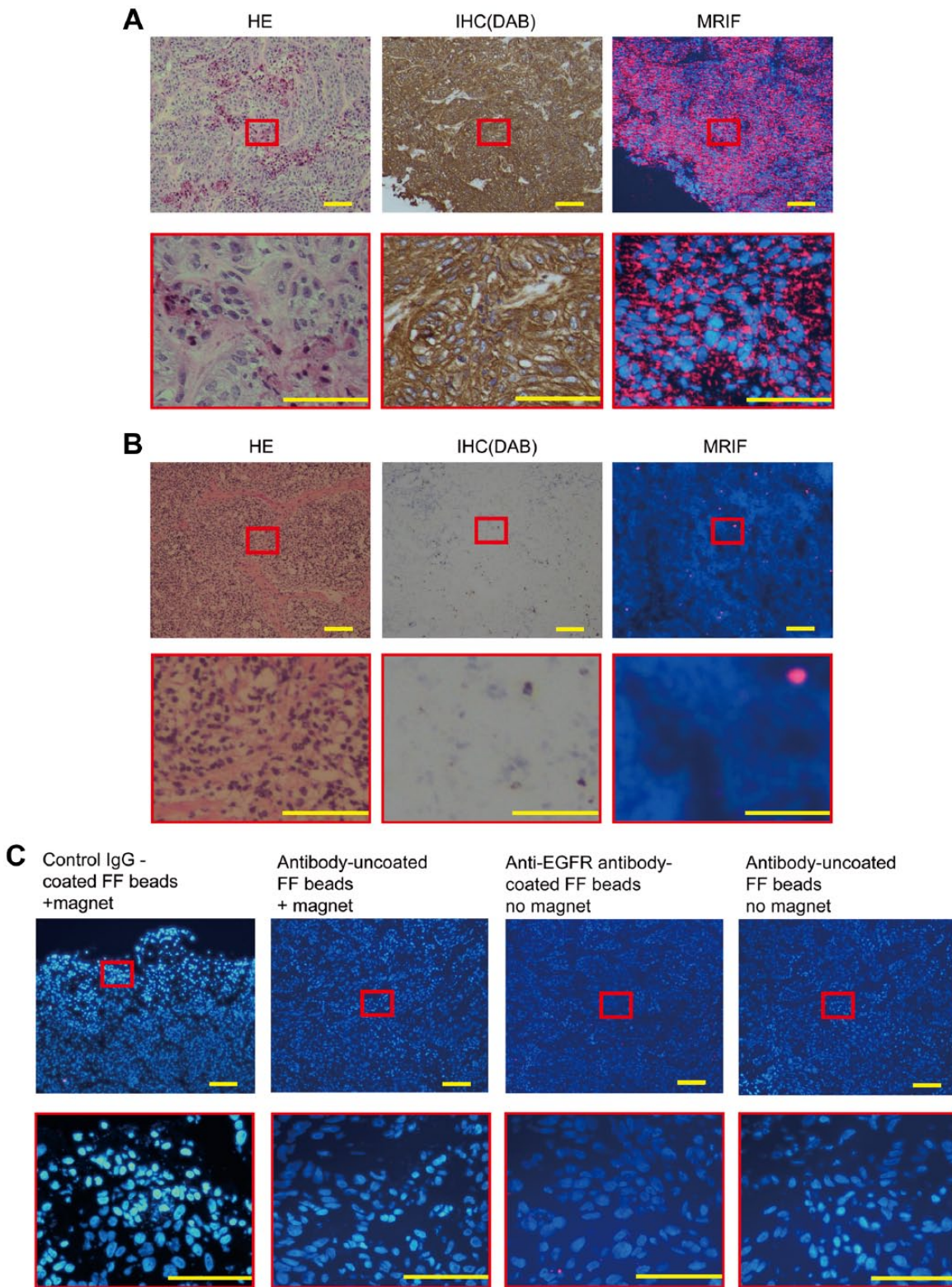


**Figure 4.** Staining of A431 cells and a lymph node by hematoxylin and eosin (HE), immunohistochemistry (IHC), and MRIF. Images of (A) A431 (human epidermoid cancer cell, high epidermal growth factor receptor [EGFR] expression) xenograft in swine and (B) normal swine lymph nodes stained with HE, IHC (diaminobenzidine, DAB), and MRIF treated with anti-EGFR antibody-coated FF beads and the magnet. (C) MRIF using IgG isotype control with a magnet, antibody-uncoated FF beads with a magnet, anti-EGFR antibody-coated FF beads without a magnet, and antibody-uncoated FF beads without a magnet. Scale bar = 100  $\mu$ m. Abbreviation: FF, fluorescent ferrite; MRIF, magnetically promoted rapid immunofluorescence.



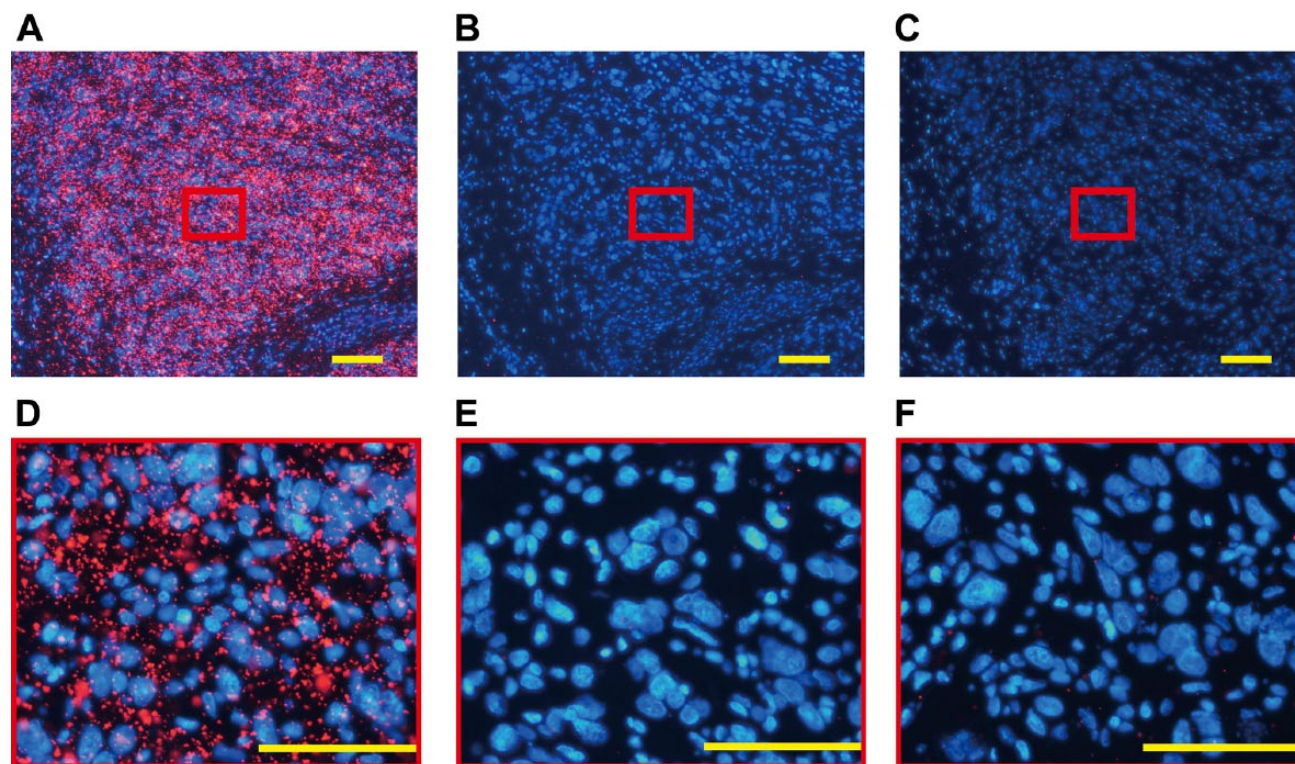


**Figure 5.** Staining of A431 cells with MRIF with a protein-blocking step before incubation. A431 cell line xenograft frozen sections were blocked with 4% skimmed milk in (A) PBS or with (B) 10 ng/ $\mu$ l or (C) 60 ng/ $\mu$ l anti-EGFR neutralizing antibody overnight before MRIF staining. Scale bar = 100  $\mu$ m. Abbreviations: PBS, phosphate buffered saline; EGFR, epidermal growth factor receptor; MRIF, magnetically promoted rapid immunofluorescence.

using the bicinchoninic acid protein assay.<sup>27</sup> To demonstrate the versatility of this method in human tissue, we examined paraffin embedded tissue arrays containing breast cancer, matched metastatic lymph nodes, and normal lymph nodes. Representative staining images of paraffin-embedded human tissue arrays containing breast cancer and metastatic lymph nodes with the MRIF and IHC methods using the anti-pan-cytokeratin antibody are shown in Fig. 6A. The areas stained with MRIF were consistent with those using IHC. Representative staining images of frozen sections of metastatic lymph nodes from breast cancer patients with the MRIF and IHC methods using the anti-pan-cytokeratin antibody are shown in Fig. 6B. The stained areas in the metastatic lymph nodes with MRIF were also consistent with those using IHC. Malignant tissue (breast carcinoma and metastatic lymph nodes) was analyzed using BRM 961, BRM961a, BRM481, and LY803. The positive rates for IHC was 96.5% (276/286) and MRIF was 92.7% (265/286). The coincidence rate was 94.8% (271/286) (Table 2). Normal tissue (i.e., breast tissue, tonsil, and lymph node) was analyzed using BRM 961, BRM961a, BRM481, LY481, and LY241e. The positive rates for IHC was 26.3% (25/95)

and MRIF was 32.6% (31/95). The coincidence rate was 91.6% (87/95) (Table 2). Frozen human metastatic lymphatic tissues were stained with both IHC and MRIF. All nodes were positive for IHC and MRIF, and the coincidence rate was 100% (6/6).

## Discussion

Intraoperative analysis of frozen tissue sections using HE staining enables diagnosis within 20 min at many institutions,<sup>28</sup> although it can be difficult to diagnose with HE staining, especially for small tumor foci in lymph nodes<sup>29,30</sup> and surgical margins.<sup>31</sup> IHC analysis is sufficient to detect small numbers of tumor cells in lymph nodes,<sup>29,30,32</sup> although a standard IHC procedure commonly requires >30 min to complete, which makes its clinical application for intraoperative diagnosis impractical. Thus, the application of new methodology for intraoperative pathological evaluation is important. We previously reported magnetically promoted rapid immune assays including enzyme-linked immunosorbent assay (ELISA) and IHC staining.<sup>17</sup> In the present study, we improved the magnetically promoted IHC procedure to a 1-min reaction and 1-min

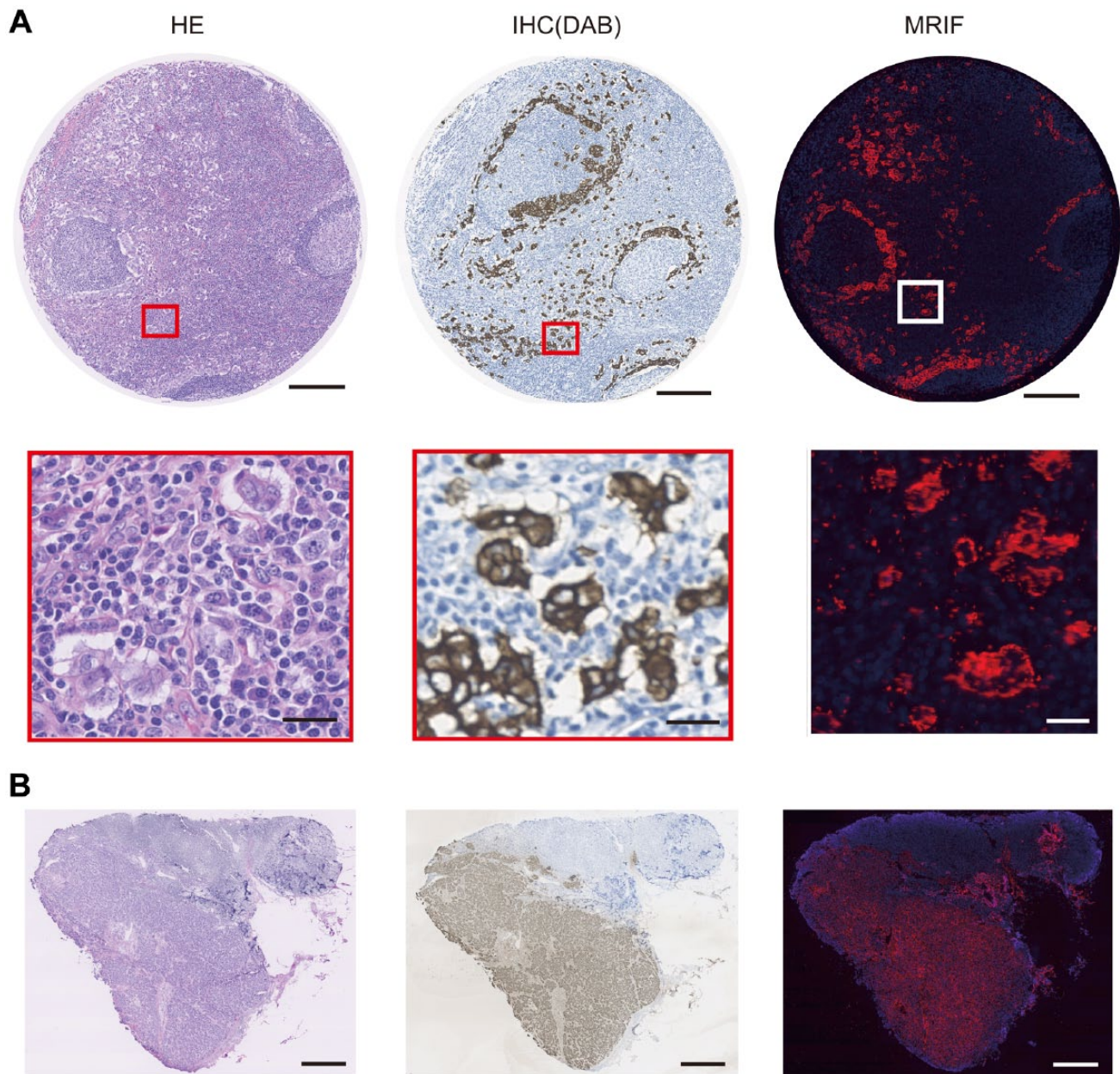


**Figure 6.** Staining image of human breast cancer metastatic lymph node by HE, IHC (DAB), and MRIF treated with anti-pan-cytokeratin antibody-coated FF beads. (A) Image of a paraffin-embedded tissue array of human breast cancer metastatic lymph node stained with HE, IHC (DAB), and MRIF. Scale bar = 250  $\mu\text{m}$  and 25  $\mu\text{m}$  for high magnification. (B) Image of frozen tissue section of human breast cancer metastatic lymph node stained with HE, IHC (DAB), and MRIF. Scale bar = 1000  $\mu\text{m}$ . Abbreviations: HE, hematoxylin and eosin; DAB, diaminobenzidine; MRIF, magnetically promoted rapid immunofluorescence; FF, fluorescent ferrite.

**Table 2.** Positive and Coincidence Rate of Immunohistochemistry and Magnetically Promoted Rapid Immunofluorescence.

	Positive Rate		Coincidence Rate
	Immunohistochemistry	Magnetically Promoted Rapid Immunofluorescence	
Malignant tissue: breast carcinoma and metastatic lymph node	96.5% (276/286)	92.7% (265/286)	94.8% (271/286)
Normal tissue: normal breast, tonsil and lymph node	26.3% (25/95)	32.6% (31/95)	91.6% (87/95)



wash for an entire method <15 min (Table 1) using frozen sections from a xenograft model and human samples. Thus, this ultra-rapid immunostaining method can provide an IHC result with sufficient speed for use during surgical operation, and may provide an ancillary method for pathological diagnosis.

Previous studies have reported rapid methods that enabled IHC procedures to be accomplished within 15 to 20 min using external energy (e.g., microwave irradiation,<sup>3,5,6</sup> alternating current electric field,<sup>12,13</sup> or ultrasound<sup>33</sup>) or immunofluorescence-labeled primary antibodies (Table 1). The mechanism by which the antigen-antibody reaction time is reduced using external energy is not fully clarified, although the stirring effect is assumed to increase the opportunity for antigens and antibodies to interact.<sup>2,3,5,6,12,13</sup> Alternatively, by using a fluorescently labeled primary antibody or a premixed primary antibody/secondary antibody, the signal amplification step can be omitted and the overall reaction time can be reduced. Micanovic et al.<sup>33</sup> described rapid immunofluorescence staining of frozen mice kidney to isolate glomeruli and proximal tubules. In that study, frozen kidney was stained with fluorescent labeled primary antibody (fluorescein isothiocyanate-phalloidin) for 3 to 5 min. Murakami et al.<sup>34</sup> reported rapid immunostaining of frozen mouse kidney to isolate the thick ascending limb, in which frozen tissues were incubated with premixed primary antibody/secondary antibody for 1 min. Hatta et al.<sup>4</sup> also reported rapid immunostaining of frozen sections of a lymph node with carcinoma invasion, in which samples were immunostained within 5 min using an immune complex of AE1/3 primary antibody and Envision-AP-conjugated secondary antibody with intermittent microwave irradiation. In the present study, the use of magnetic force attracts the FF beads and reduces the immune reaction between the antibody-coated FF beads and the antigens. Furthermore, fluorescent reagents were contained within the FF beads, which eliminates the signal amplification step and decreases the overall reaction time. However, the fixation and blocking times of this method are longer than other methods (Table 1) and these steps should be improved.

The FF bead consists of ferrite (magnetic iron oxide) particles and europium and emits bright red fluorescence under UV irradiation. Europium is not restricted to encapsulation of a single substance. We are currently developing multicolor staining by encapsulating various types of hydrophobic fluorescent substances, such as dipyrromethene dyes, and attaching corresponding antibodies. Multicolor staining can then be performed using other substances. The mechanism of action of our system involves drawing the ferrites to the sample

surface by magnetic force, which accelerates the contact between the antigens and antibodies (Fig. 1). This is a direct detection method, rather than the more widely used indirect methods. The reaction is rapid and the steps are simple, which reduces the time to complete the assay. A common disadvantage of direct methods is the low signal resulting from the 1:1 ratio of antibody fluorescence to enzyme conjugation, when compared with the multiple signal amplification steps in indirect methods. However, our FF beads contain  $>3.0 \times 10^5$  molecules of fluorescence per bead, which provide sufficient brightness to overcome this disadvantage. One of the limitations of immunofluorescence, as well as this method, is the lack of contextual histo- and cytoplasmic-morphological features. To overcome this problem, morphological evaluation of sequential HE specimen by pathologist is still required.

We investigated the staining and washing conditions using EGFR-positive xenograft samples, and then optimized conditions in clinical samples with the pan-cytokeratin antibody. Our method was sufficient for detection of both EGFR and pan-cytokeratin. Target retrieval with proteinase was required for pan-cytokeratin. The actual binding time of the antibody/antigen can vary considerably depending on the antibody, antigen, tissue, and fixation. Thus, further studies examining the utility of our method with different conditions, targets, and antibodies are required. With respect to the false negatives and false positives found in the tissue arrays, these are likely related to insufficient reaction and washing times. Furthermore, all processes in the present study, including incubation and washing of FF beads, were done manually, which may have resulted in non-uniform staining and inadequate washing. Automating the system may solve such problems. The optimal magnetic force for antibody reaction and washing is a critical factor in our technique. MRIF staining was only achieved when the magnetic force between the sample and magnet was optimal. As the magnetic forces are unequally distributed across the surface of the magnet, agitation of the sample (or magnet) was employed to achieve more uniform staining. We are in the process of automating this system for more practical use.

In summary, we successfully developed an MRIF system for frozen sections of xenograft and human tissue using antibody-coated FF beads containing ferrites and fluorophores. The magnet accelerates the binding between the sample and FF beads, and reduces the time to immunoassay completion. The attached FF beads can be viewed under a fluorescent microscope without extra signal amplification. This ultra-rapid immunostaining method, when used under optimal conditions, may provide an ancillary technique for pathological diagnosis during surgery.

## Acknowledgments

Dr. Fumihiko Ishikawa (RIKEN Center for Integrative Medical Sciences, Yokohama, Kanagawa) and the staff of Prime Tech Ltd. (Tsuchiura, Ibaraki, Japan) contributed to the development of RAG2 knockout swine. We thank Professor David Heery (The Nottingham University) for his support, the Collaborative Research Resources, School of Medicine, Keio University for technical assistance, and Edanz Group ([www.edanzediting.com/ac](http://www.edanzediting.com/ac)) for editing a draft of this manuscript.

## Competing Interests

The author(s) declared the following potential conflicts of interest with respect to the research, authorship, and/or publication of this article: Fluorescent ferrite beads can be purchased from Tamagawa Seiki Co. Ltd., and H.Y. and N.H. belong to Tamagawa Seiki Co. Ltd. The other authors declare they have no competing interests.

## Author Contributions

All authors contributed to this article. SM and YN designed the experiments; JK and KK evaluated pathological images; AT, SSakamoto, and HH provided antibody-coated functionalized fluorescent ferrite beads; SSuzuki, DF, and AO provided recombination activating gene 2 knockout swine; SC, MKaneko, AK, and MS calculated the magnetic forces; HY and NH provided the jig; TO and YN performed the experiments; TH, HJ, MKusakabe, and YK interpreted the results; TK, HT, TS, KT, and SN provided and evaluated the clinical samples; and TO and SM wrote the manuscript. All authors have read and approved the manuscript as submitted.

## Funding

The author(s) disclosed receipt of the following financial support for the research, authorship, and/or publication of this article: This research was supported by the Project for Medical Device Development from Japan Agency for Medical Research and Development, AMED under Grant Number JP18he0902010h0004.

## Literature Cited

1. Taylor CR, Cote RJ. Immunomicroscopy: a diagnostic tool for the surgical pathologist. 3rd ed. Philadelphia: Saunders; 2006.
2. Choi YJ, Yun HR, Yoo KE, Kim JH, Nam SJ, Choi YL, Ko YH, Kim BT, Yang JH. Intraoperative examination of sentinel lymph nodes by ultrarapid immunohistochemistry in breast cancer. *Jpn J Clin Oncol*. 2006;36:489–93.
3. Hatta H, Tsuneyama K, Kondo T, Takano Y. Development of an ultrasound-emitting device for performing rapid immunostaining procedures. *J Histochem Cytochem*. 2010;58:421–8.
4. Hatta H, Tsuneyama K, Kumada T, Zheng H, Cheng C, Cui Z, Takahashi H, Nomoto K, Murai Y, Takano Y. Freshly prepared immune complexes with intermittent microwave irradiation result in rapid and high-quality immunostaining. *Pathol Res Pract*. 2006;202:439–45.
5. Jylling AM, Lindebjerg J, Nielsen L, Jensen J. Immunohistochemistry on frozen section of sentinel lymph nodes in breast cancer with improved morphology and blocking of endogenous peroxidase. *Appl Immunohistochem Mol Morphol*. 2008;16:482–4.
6. Kumada T, Tsuneyama K, Hatta H, Ishizawa S, Takano Y. Improved 1-h rapid immunostaining method using intermittent microwave irradiation: practicability based on 5 years application in Toyama Medical and Pharmaceutical University Hospital. *Mod Pathol*. 2004;17:1141–9.
7. Leong AS, Daymon ME, Milios J. Microwave irradiation as a form of fixation for light and electron microscopy. *J Pathol*. 1985;146:313–21.
8. Matsumoto M, Natsugoe S, Ishigami S, Uenosono Y, Takao S, Aikou T. Rapid immunohistochemical detection of lymph node micrometastasis during operation for upper gastrointestinal carcinoma. *Br J Surg*. 2003;90:563–6.
9. Monig SP, Luebke T, Soheili A, Landsberg S, Dienes HP, Holscher AH, Baldus SE. Rapid immunohistochemical detection of tumor cells in gastric carcinoma. *Oncol Rep*. 2006;16:1143–7.
10. Nahrig JM, Richter T, Kuhn W, Avril N, Flatau B, Kowolik J, Hoffer H, Werner M. Intraoperative examination of sentinel lymph nodes by ultrarapid immunohistochemistry. *Breast J*. 2003;9:277–81.
11. Richter T, Nahrig J, Komminoth P, Kowolik J, Werner M. Protocol for ultrarapid immunostaining of frozen sections. *J Clin Pathol*. 1999;52:461–3.
12. Salem AA, Douglas-Jones AG, Sweetland HM, Mansel RE. Intraoperative evaluation of axillary sentinel lymph nodes using touch imprint cytology and immunohistochemistry: I. Protocol of rapid immunostaining of touch imprints. *Eur J Surg Oncol*. 2003;29:25–8.
13. Terata K, Saito H, Nanjo H, Hiroshima Y, Ito S, Narita K, Akagami Y, Nakamura R, Konno H, Ito A, Motoyama S, Minamiya Y. Novel rapid-immunohistochemistry using an alternating current electric field for intraoperative diagnosis of sentinel lymph nodes in breast cancer. *Sci Rep*. 2017;7:2810.
14. Toda H, Minamiya Y, Kagaya M, Nanjo H, Akagami Y, Saito H, Ito M, Konno H, Motoyama S, Ogawa J. A novel immunohistochemical staining method allows ultrarapid detection of lymph node micrometastases while conserving antibody. *Acta Histochem Cytochem*. 2011;44:133–9.
15. Tsutsumi Y, Serizawa A, Kawai K. Enhanced polymer one-step staining (EPOS) for proliferating cell nuclear antigen (PCNA) and Ki-67 antigen: application to intraoperative frozen diagnosis. *Pathol Int*. 1995;45:108–15.
16. Viberti L, Croce S, Pecchioni C, Bongiovanni M, Sapino A. [Rapid immunohistochemistry applied to intraoperative diagnosis: a critical analysis]. *Pathologica*. 2001;93:544–8.
17. Tanino M, Sasajima T, Nanjo H, Akesaka S, Kagaya M, Kimura T, Ishida Y, Oda M, Takahashi M, Sugawara T, Yoshioka T, Nishihara H, Akagami Y, Goto A, Minamiya Y, Tanaka S. Group RIS rapid immunohistochemistry based on alternating current electric field for intraop-



- erative diagnosis of brain tumors. *Brain Tumor Pathol.* 2015;32:12–9.
18. Sakamoto S, Omagari K, Kita Y, Mochizuki Y, Naito Y, Kawata S, Matsuda S, Itano O, Jinno H, Takeuchi H, Yamaguchi Y, Kitagawa Y, Handa H. Magnetically promoted rapid immunoreactions using functionalized fluorescent magnetic beads: a proof of principle. *Clin Chem.* 2014;60:610–20.
  19. De Luca A, Carotenuto A, Rachiglio A, Gallo M, Maiello MR, Aldinucci D, Pinto A, Normanno N. The role of the EGFR signaling in tumor microenvironment. *J Cell Physiol.* 2008;214:559–67.
  20. Ozawa S, Ueda M, Ando N, Abe O, Hirai M, Shimizu N. Stimulation by EGF of the growth of EGF receptor-hyperproducing tumor cells in athymic mice. *Int J Cancer.* 1987;40:706–10.
  21. Ozawa S, Ueda M, Ando N, Abe O, Shimizu N. High incidence of EGF receptor hyperproduction in esophageal squamous-cell carcinomas. *Int J Cancer.* 1987;39:333–7.
  22. Suzuki S, Iwamoto M, Hashimoto M, Suzuki M, Nakai M, Fuchimoto D, Sembon S, Eguchi-Ogawa T, Uenishi H, Onishi A. Generation and characterization of RAG2 knockout pigs as animal model for severe combined immunodeficiency. *Vet Immunol Immunopathol.* 2016;178:37–49.
  23. Hatakeyama M, Mochizuki Y, Kita Y, Kishi H, Nishio K, Sakamoto S, Abe M, Handa H. Characterization of a magnetic carrier encapsulating europium and ferrite nanoparticles for biomolecular recognition and imaging. *J Magn Magn Mater.* 2009;321:1364–7.
  24. Guan JB, Chen B, Sun YY, Liang H, Zhang QJ. Effects of synergetic ligands on the thermal and radiative properties of Eu(TTA)(3)nL-doped poly(methyl methacrylate). *J Non-Cryst Solids.* 2005;351:849–55.
  25. Nishio K, Masaike Y, Ikeda M, Narimatsu H, Gokon N, Tsubouchi S, Hatakeyama M, Sakamoto S, Hanyu N, Sandhu A, Kawaguchi H, Abe M, Handa H. Development of novel magnetic nano-carriers for high-performance affinity purification. *Colloids Surf B Biointerfaces.* 2008; 64:162–9.
  26. Sakamoto S, Hatakeyama M, Ito T, Handa H. Tools and methodologies capable of isolating and identifying a target molecule for a bioactive compound. *Bioorg Med Chem.* 2012;20:1990–2001.
  27. Smith PK, Krohn RI, Hermanson GT, Mallia AK, Gartner FH, Provenzano MD, Fujimoto EK, Goeke NM, Olson BJ, Klenk DC. Measurement of protein using bicinchoninic acid. *Anal Biochem.* 1985;150:76–85.
  28. Novis DA, Zarbo RJ. Interinstitutional comparison of frozen section turnaround time. A College of American Pathologists Q-Probes study of 32868 frozen sections in 700 hospitals. *Arch Pathol Lab Med.* 1997;121:559–67.
  29. Giuliano AE, Dale PS, Turner RR, Morton DL, Evans SW, Krasne DL. Improved axillary staging of breast cancer with sentinel lymphadenectomy. *Ann Surg.* 1995;222:394–9; discussion 399–401.
  30. Turner RR, Ollila DW, Krasne DL, Giuliano AE. Histopathologic validation of the sentinel lymph node hypothesis for breast carcinoma. *Ann Surg.* 1997;226: 271–6; discussion 276–8.
  31. Moncrieff MD, Shah AK, Igali L, Garioch JJ. False-negative rate of intraoperative frozen section margin analysis for complex head and neck nonmelanoma skin cancer excisions. *Clin Exp Dermatol.* 2015;40:834–8.
  32. Nowikiewicz T, Srutek E, Zegarski W. Application of immunohistochemistry for detection of metastases in sentinel lymph nodes of non-advanced breast cancer patients. *Pol J Pathol.* 2015;66:22–9.
  33. Micanovic R, Khan S, El-Achkar TM. Immunofluorescence laser micro-dissection of specific nephron segments in the mouse kidney allows targeted downstream proteomic analysis. *Physiol Rep.* 2015;3:e12306.
  34. Murakami H, Liotta L, Star RA. IF-LCM: laser capture microdissection of immunofluorescently defined cells for mRNA analysis rapid communication. *Kidney Int.* 2000;58:1346–53.